Ray racing techniques applied to modelling of fluorescent solar collectors

T.J.J. Meyer*[a], J. Hlavaty[b], L. Smith[c], E.R. Freniere[b], T. Markvart[a]
[a]Solar Energy Laboratory, University of Southampton, UK SO171BJ
[b]Lambda Research Corporation, 80 Taylor Street, Littleton, Massachusetts, MA USA 01460
[c]Ceres, 315 Webster Street, Needham, MA USA 02494

ABSTRACT

Fluorescent solar collectors represent an alternative to flat plate photovoltaic arrays. With the emphasis on minimizing the use of silicon, the collector is usually composed of a mixture of fluorescent dyes embedded in a transparent medium. The absorbed incoming sunlight is re-emitted at a longer wavelength. A large fraction of fluorescence is totally internally reflected and transported to the edge of the collector, where the solar cell is placed. The key requirements for efficient fluorescent collectors are a good photon transport and a broad absorption of sunlight. The fundamental parameter that determines the efficiency of photon transport is the probability of reabsorption.

Based on experimental results and ray-tracing simulations carried out with "TracePro", this publication illustrates the use of ray tracing to model reabsorption in collectors with different shapes as well as inhomogeneous structures, and to assess the validity of the traditional analytical approach. We show that, contrary to expectations, some novel structures (for example, "thin film" or "waveguide" collectors) do not represent an improvement over their corresponding homogeneous collectors and that any variation of the film refractive index on a glass substrate leads to an efficiency drop.

Keywords: Fluorescence, Solar Collector, Optical Design, Fluorescence Solar Collector, Ray tracing, Solar Energy

1. INTRODUCTION

Fluorescent **S**olar **C**ollectors (FSCs) for solar energy conversion represent an attractive photovoltaic technology as they have the potential to decrease substantially the size of solar cells, thereby reducing the overall system cost [1].

In conventional FSC devices, the collector (absorber) is generally composed of a mixture of fluorescent dyes embedded in a transparent medium such as PMMA, glass or even a liquid solution (Fig. 1). When exposed to sunlight, the dye absorbs a part of the incoming light and re-emits photons inside the fluorescent layer at a longer wavelength. Efficient photon collection at the edge solar cell is achieved since most of the fluorescent light is re-emitted at more oblique angles to the surface than the critical angle for total internal reflection

An important factor for making a good FSC device consists of a broad absorption of the incident light by using an appropriate mix of dyes. At the same time, it is important to ensure that the mix of fluorophores emits in an absorption free region [2]. Ideally, the emission region is spectrally narrow [3] and as close as possible to the semiconductor band gap (λ_g) in order to preserve an optimal absorption of the daylight.

In practice, increasing the dye concentration for efficient day light absorption decreases the FSC efficiency since it increases re-absorption occurring from an overlap of the fluorescence and absorbance bands. We may also note that, by Kirchhoff's law, the absorption and fluorescence bands of a given fluorophore are interconnected through thermodynamics [4] and it is impossible to create a window completely free form absorption in a system which absorbs and emits light [2-3].

Physics and Simulation of Optoelectronic Devices XVII, edited by Marek Osinski, Bernd Witzigmann, Fritz Henneberger, Yasuhiko Arakawa, Proc. of SPIE Vol. 7211, 72110N · © 2009 SPIE · CCC code: 0277-786X/09/$18 · doi: 10.1117/12.810922

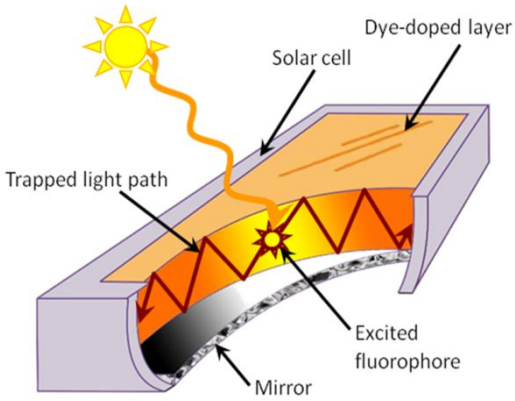

Fig. 1. Cut away of a fluorescent solar collector showing the large area A_{front} of the fluorescent medium (orange) exposed to sunlight and the solar cells (grey) with an area A_{edge} placed at the edge of the collector. The optical gain G of these devices is equal to the ratio A_{front}/A_{edge}.

Re-absorption of fluorescence is known to be the key factor limiting the collector's efficiency; in example, for a glass collector the photon collection probability on the edge solar cell drops by about a half within four re-absorption events [1-2, 5]. Thin film designs (also known as waveguide designs), i.e. a thin film containing dye coated on a clear substrate where the refractive index of the film can differ from the substrate, were suggested for an improvement of the photon transport capabilities. However, as we shall show, these structures can achieve at best the collection efficiency of their corresponding homogeneous collector.

The aims of this paper are to assess the potential of thin film designs by modelling the re-absorption probability using a commercial ray tracing software (TracePro) and to compare the simulations with experimental results.

An original type of collectors, "liquid collectors", based on a thin glass cuvette which contains the fluorescent solution, was introduced to mimic different thin film devices where the walls of the cuvette serve as clear substrate. In addition, the simplicity of replacing the fluorescent solution allows easy variation of the matrix refractive index.

The ray tracing simulation and the experimental results show that thin film collectors are analogous to standard collectors when the refractive index of the fluorescent layer matches that of the substrate and that variation in refractive index lead to an efficiency drop.

2. LIMITS OF THE CURRENT TECHNOLOGY

The principles of operation of FSCs can be understood by following the **W**eber and **L**ambe model (*W&L*) [1]. In this model the optical efficiency, the fraction of incident photons that illuminate the solar cell, of a collector (η_{FSC}) is given by the product of two factors:

$$\eta_{FSC} = Q_a \times Q_c \tag{1}$$

where Q_a is the absorption efficiency and Q_c is the collection efficiency.
The absorption efficiency Q_a is defined as the fraction of incident photons absorbed in the collector whilst the collection efficiency Q_c stands for the fraction of photons transported in the y direction reaching the solar cell at $y=L$ (Fig. 2).

Including only photons above the semiconductor band gap λ_g; the absorption efficiency Q_a can be defined as:

$$Q_a = \int_0^{\lambda_g} \dot{F}(\lambda)(1-\exp(-\alpha l)\, d\lambda \Big/ \int_0^{\lambda_g} \dot{F}(\lambda)\, d\lambda \tag{2}$$

where $\dot{F}(\lambda)$ is the incident photon flux , l is the thickness of the collector and α the absorption coefficient.

The collector geometry usually considered in the analytical treatment represents an infinite strip along the x direction, with perfect mirror at $y = 0$, as shown in Fig. 2 [1-2].

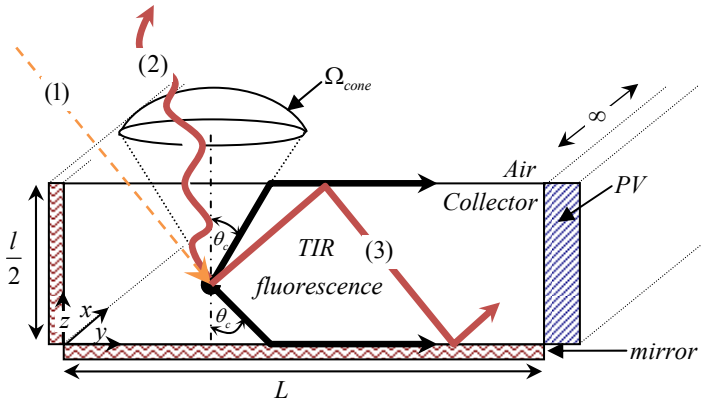

Fig. 2. The cross section of FSC considered in [1-2] showing the escape cone at the interface air/collector

The sun ray incident on the front surface of the collector (1) is absorbed by the dye. Light is subsequently emitted at a longer wavelength by the fluorophore in a random direction. The outcome of the ray depends on the angle of re-emission; if the light is emitted in a shallow angle $<\theta c$ the fluorescence escapes from the top of the collector (2), if the light is re-emitted at oblique angles $>\theta c$ the fluorescence is trapped (TIR) (3).
After a re-absorption/re-emission event, the probability P that an emitted photon will escape from a collector is:

$$P = \frac{\Omega_c}{4\pi - \Omega_c} = \left(1 - \frac{1}{n_{col}^{\,2}}\right)^{1/2} = \cos(\theta_c) \tag{3}$$

where n_{col} is the refractive index of the collector.

Weber and Lambe [1] offered a simple model for Q_c^1 in terms of a single re-absorption/re-emission event of the fluorescent photon:

$$Q_c^1 = \phi(1-P)(1-R) \tag{4}$$

where R is given by the Beer-Lambert law over the path length of photons trapped within the collector:

$$R(L,\alpha,P) = \frac{\int_0^L \int_0^{\pi} \int_{\theta_c}^{\pi-\theta_c} \left(\exp^{\frac{-\alpha(L-y)}{\sin(\theta)\sin(\vartheta)}} + \exp^{\frac{-\alpha(L+y)}{\sin(\theta)\sin(\vartheta)}} \right) \sin(\theta) d(\theta) d(\phi) d(y)}{4\pi LP} \tag{5}$$

where ϕ and θ are the usual spherical coordinates defining the directions of emission.

The W&L model assumes a uniform distribution of the excited molecules throughout the collector, perfectly flat specular reflecting surfaces, no scattering of light inside the collector and no absorption of light except by the dye. In essence, relation (4) gives the collection efficiency for the first generation of photons, that is the fraction of photons reaching the solar cell after a single absorption/emission event, as indicated by the superscript 1 of Q_c^1 - in other words, as soon as a photon is absorbed it is considered as lost. In reality, the first generation photons can be re-absorbed and re-emitted, becoming second generation photons, with a possibility to be collected. Therefore, Q_c can be obtained by summing a geometric series of terms corresponding to re-absorption events [6-7] or simply by considering the balance between photon absorption and emission in the collector [2].

$$Q_c = \frac{\phi(1-P)(1-R)}{1-[(1-P)R]\phi} \tag{6}$$

Relation (6) stresses the fundamental limitation imposed by the re-absorption loss. If the optical density of the collector is increased to enhance the absorption of the incident radiation, the collection efficiency decreases. Clearly, the efficiency of a collector mainly depends on the re-absorption probability.

3. MODELLING OF THE RE-ABSORBTION PROBABILITY BY RAY TRACING

In this section the re-absorption model of Weber and Lambe [1] is verified against ray tracing simulation techniques and the limitations of the model are studied. The re-absorption probability for different geometries and for thin film collectors are studied and compared to standard homogeneous collectors.

3.1 Implementation of the Weber and Lambe model in TracePro

The infinite ribbon geometry used in the *W&L* model was reproduced in the ray tracing software by using two perfect reflectors placed in the *xy* plane. The collector studied was *50 mm x 50 mm* wide, and its thickness varied to change the gain. The refractive index of the collector was set to $n_{col}=1.5$ and the surfaces of the mirrors of the collector were perfectly flat; each mirror had perfect reflectivity. Following the assumptions of *W&L* the re-absorption probability was modelled using three different approaches. The first one, using the concept of infinite geometry, consisted in placing point sources, emitting in *4π sterad*, uniformly spaced on the symmetry *y* axis (Fig. 2). The second approach consisted in filling up the volume of the collector with $1x10^6$ sources, which were placed either uniformly or using a Monte Carlo algorithm. The third technique used the fluorescence built in algorithm of TracePro. The collector was uniformly illuminated with $1x10^6$ rays normal to the surface the wavelength of the incident rays corresponded to the maximum absorption of the fluorophore. The position of the absorption/emission event was randomly selected along the excitation wavelength ray path, from when the ray enters the fluorescing object to when it exits; the fluoresced ray direction was arbitrarily chosen over *4π sterad*. The re-absorption probability, for the three techniques, was then obtained by counting the numbers of photons reaching the edge solar cell. The comparisons between the analytical equation (5) and the ray tracing simulation are shown in Fig. 3.

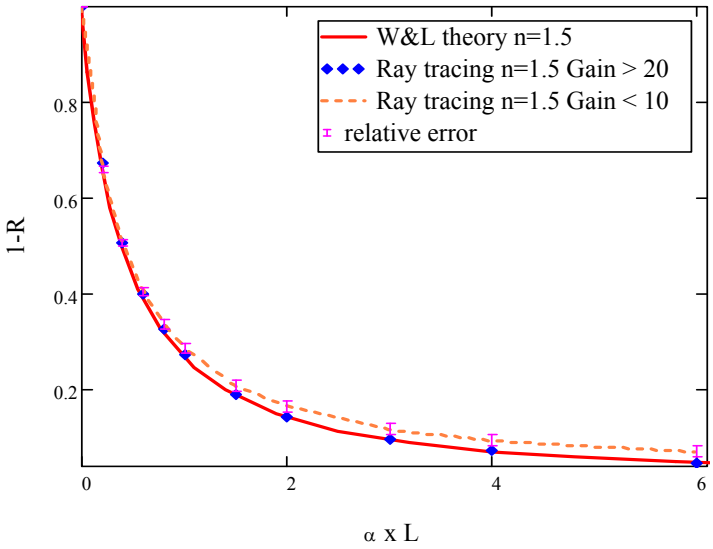

Fig. 3. Re-absorption probability analytically computed through (Eq. 5) for a collector with a refractive index *n=1.5* (red line) compared to the ray tracing simulation computed for different collector gain refractive index

Similar results were obtained for the re-absorption probability modelled with these three approaches; these also agreed (within 1%) with the *W&L* model. Variations of the collector gain showed the limitations of the analytical model for a small gain (Fig. 3). The discrepancy between the analytical model and ray tracing simulations are negligible for a gain greater than 20. The effect of the collector refractive index was also studied and it was found that it has little impact on the re-absorption probability.

The other assumptions linked to relation (5) imply perfect optical interfaces. The re-absorption probability for the same collector configuration (gain > 20) was re-computed for an arrangement of standard quality mirrors rather than perfect mirrors. The specular coefficient of the modelled mirrors was set to *0.95* with *5 %* absorptance; light scattering was modelled using the bidirectional scattering distribution function (*BRDF*) [8] and the Harvey-Shack "*shift invariant*" approximation [9] for scattering, which is mainly due to remaining surface roughness after polishing. The BRDFA, B and g coefficients were equal to 0.0001, 0.15 and 2, respectively leading to a 0.13% gaussian scatter distribution. Fig. 4 illustrates the effect of a poor choice of optics affecting the TIR photon transport.

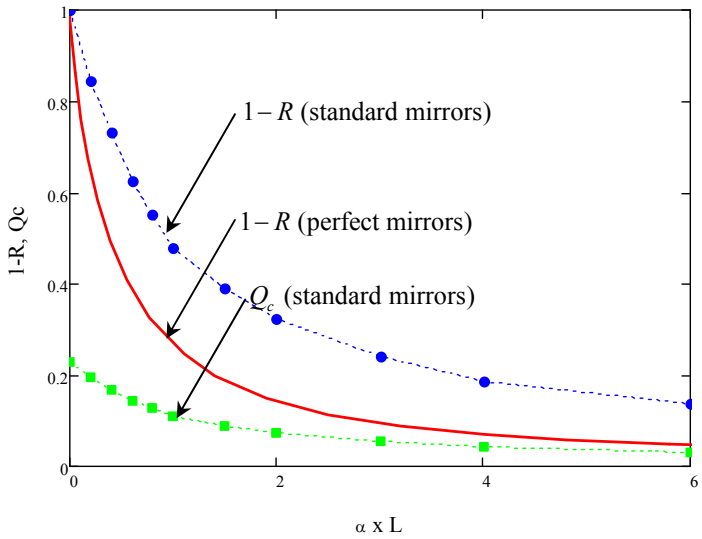

Fig. 4. Effect of light scattering on the re-absorption probability and photon collection efficiency. The refractive index of the collector modelled is equal to 1.5

The ray tracing results show that both the re-absorption probability and the probability of photon loss in the escape cone are affected by light scattering. Compared to a collector with perfect interfaces, the results shown in Fig. 4 indicate that the probability of photon loss in the escape cone increases by a factor of about 3. Hence, the photon collection efficiency dramatically decreases for collectors with rough surfaces (shown by the green curve Fig. 4). This scattering effect was negligible in all the collectors that were studied experimentally (Secs. 4 and 5) on account of highly polished surface, to [10].

3.2 Influence of the collector geometry

The re-absorption probability for collectors with different shapes was computed using the same techniques as explained in section 3.1. The collectors studied were in the shapes of square, half-disk, triangular, and ¼ disk. The area of the edge solar cell (*50 mm²*) and the volume of the collector (*2500 mm²*) were the same in all of the designs, giving the same gain for all the structures. The details of the collector geometry are shown in Table. 1.

Table. 1. Different geometry studied by ray tracing simulations, the letter ℜ indicates a perfect reflector

Shape	*Dimensions (mm)*	*Shape*	*Dimensions (mm)*
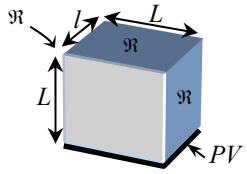	*square collector* $L = 50$ $l = 1$ $G = 50$	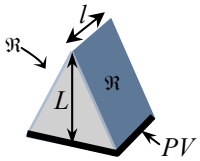	*triangle collector* $L = 100$ $l = 1$ $G \approx 50$
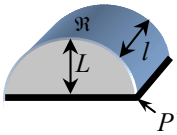	*½ disk collector* $L = 39.9$ $l = 1$ $G \approx 50$	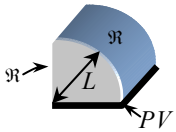	*¼ disk collector* $L = 56.42$ $l = 1$ $G \approx 50$

Fig. 5 shows the re-absorption probability as a function of the product αL for different collector shapes. The probability of photons escaping in the critical cone is the same for all the collectors studied; hence the re-absorption probability in this graph is directly related to the collection efficiency.

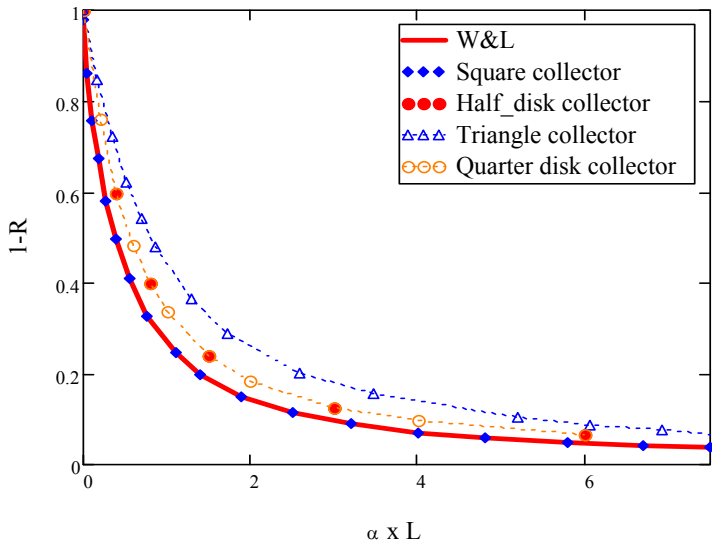

Fig. 5. Re-absorption probability for different geometrical shapes

The use of perfect mirrors to mimic infinite structures is proven to be a valid argument since the re-absorption probability of the square collector (see Table. 1) agrees perfectly with the *W&L* model; therefore, any symmetrical shape which can be unfolded with the use of a perfect reflector (e.g. half disk and quarter disk or equilateral triangles and hexagonal geometry) will have the same re-absorption probability. Figure 5 clearly shows that the triangle geometry is the most efficient shape to reduce re-absorption losses. These results are consistent with the analytical theory developed by Goetzberger [11].

3.3 Influence of the collector homogeneity

In addition to the homogeneous collectors discussed in Sec. 3.2, we have also considered the re-absorption probability of thin film and liquid collectors and compared the results to the *W&L* model. These devices are inhomogeneous since they are characterised by more than one refractive indices. Details of the inhomogeneous collectors modelled are given in Table. 2.

Table. 2. Inhomogeneous collectors studied by ray tracing simulations. The letter $\Re$ indicates a perfect reflector

Shape	*Dimensions (mm)*	*Shape*	*Dimensions (mm)*
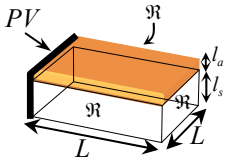	*Thin film* $L = 50$ $l_s = 1, l_a = 0.001$ $G \approx 50$	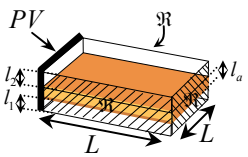	*liquid collector* $L = 50$ $l_a = 0.25, l_s = l_1 + l_2 = 0.25$ $G = 50$

We have shown in [2] that, for practical purposes, the re-absorption probability of thin film and liquid collectors are the same as for homogeneous collectors with the refractive index of the absorbing layer n_a of thickness l_a equal to the refractive index of the transparent substrate n_s, with total thickness l_s if the homogeneous collectors has an effective absorption coefficient α_{eff} equal to:

$$\alpha_{eff} = \alpha \frac{l_a}{l_s + l_a} \tag{7}$$

where α is the absorption coefficient of the absorbing layer.
Relation (7) can justified by a simple geometrical consideration of the optical path of the rays emitted by the dye that reach the edge of the collector [2] which are generally reflected many times from the front and rear surfaces along their path. The comparison between the ray tracing simulations and the *W&L* model is shown in Fig. 6.

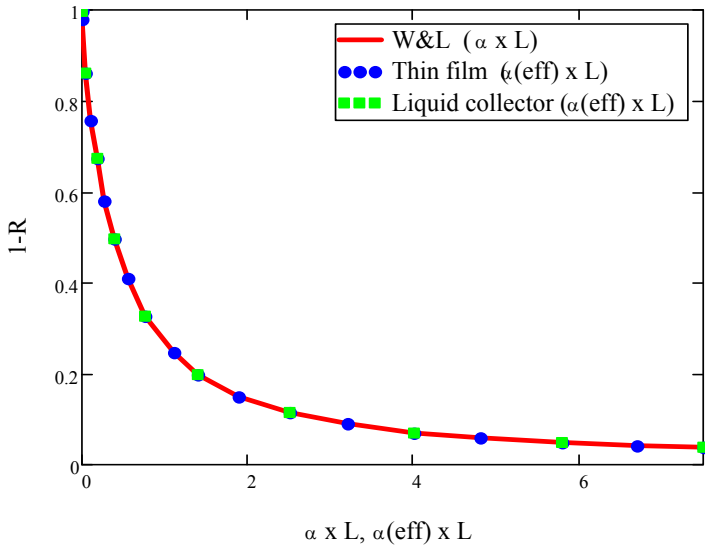

Fig. 6. Re-absorption probability for thin film and liquid collectors compared to the *W&L* model

This result shows that an inhomogeneous (or thin film) collector with $n_a=n_s$, is equivalent to a homogeneous collectors with the same geometry and with the same absorption efficiency.
In such systems the refractive index of the substrate can of course be changed, but before assessing the "wave guiding" potential of these possible variations we turn towards the experimental side to validate the results obtained with TracePro.

4. EXPERIMENTAL DETAILS

Thin film collectors and liquid collectors doped with different dyes were fabricated to verify the results obtained by ray tracing. The fabrication and characterisation procedures are detailed below.

4.1 Material and sample preparation

The thin film collectors were prepared by spin coating of dye-polymer solutions onto polished square glass substrates (*Menzel 26 mm x 26 mm x 1mm*, clear cut edges) [12]. The thickness of the film, Tensol 12 doped with Rhodamine 6G (*R6G, Ø=0.95*) was measured by using a profilometer type Taylor-Hobson Talysurf-120 L and found to be $\approx 10\mu m$ [2].
The near-matching refractive indexes of the Tensol film (*1.48*) and glass slide (*1.51, sodium D-line, 589 nm*) allowed the thin film collector to be treated as homogeneous.

The liquid collector used in this work was similar to a "stretched" spectroscopic cuvette; a quartz cell of optical dimensions *50 mm x 50 mm* with a spacing of 0.5 *mm* was filled with a solvent. This quartz cuvette (*SUPRAZIL n=1.46*) with walls *1mm* thick was fabricated by Hellma-Germany. All the structural parts were polished and formed a homogeneous structure through contacts produced via a direct fuse process. An atomic force microscope (*MFP-3D AFM Asylum Research UK*) determined the average roughness of the quartz cuvette ≈ *6 nm* ensuring good photon propagation through total internal reflection.
The spectroscopic studies on the liquid collectors were carried out using *R6G*, Rhodamine 101 (*R101, Ø=1*) with properties well documented in the literature [13], as well as new Lumogen dyes from BASF Frot 305 (*F305, Ø=0.95*[14]). Dichloromethane (*DCM*) was the solvent used for studying the Frot 305 dye because its refractive index is equal to 1.42 which is close to the quartz refractive index. This measure prevents optical mismatch at the quartz/ liquid interface whereas ethanol was used as solvent for the Rhodamine dyes. In addition, the temperature of the solution was kept under control throughout the experiment to reduce evaporation.

A silicon solar cell was coupled to one edge of the sample creating a working device. Mirrors surrounding the samples were mimicking the infinite strip geometric configuration of W&L [1]; the mirrors used were ¼ wavelength first surface mirrors (*Edmund optic*) with a reflectivity > *90%* across the visible spectrum cut to the specific dimension using a

precision diamond saw or high reflective film (*3M Vikuiti enhanced specular reflector*); an air gap $\approx 10\ \mu m$ was always left between the mirrors and the collectors.

4.2 Spectroscopic measurements

The instruments used for all absorption and fluorescence measurements were an Avantes spectrometer (*AvaSpec-2048, grating UA (200-1100 nm), slits 25 μm*) based on the symmetrical Czerny-Turner design with a *2048* pixel CCD detector array, or a Bentham spectrometer equipped with a monochromator (*TM300)* and a PMT tube (*Hamamatsu R446*), or a calibrated silicon detector (*dh_Si, Bentham Instruments Ltd*)..
The absorbance spectra were measured in a standard fashion, with the fibre placed at the back in the centre of the collector. The edge fluorescence setup was a standard *90* degrees angle detection of fluorescence.

The illumination setup was different for the two devices: thin film collectors were directly placed in a solar simulator (*T.S. Space Systems*) equipped with a Xenon lamp approximating *AM1.5*. On the other hand, the liquid collectors were uniformly illuminated by a Bentham (*CL2*) universal spectral irradiance standard lamp (*calibration traceable to NPL Teddington, UK*) with a wavelength range *250 nm* to *3000 nm* and a colour temperature of *3270 K* because the heat conveyed by the strong *AM 1.5* illumination was not suitable for the volatile solvent used in this type of collector. The distance between the lamp and the collector was *26.5 cm* and all the measurements took place in a light proof black box.

5. RESULTS

The methodology used in this paper to determine the re-absorption probability of the samples studied was reviewed in [2] and rests on the comparison between the fluorescence spectrum of the dye which are free from re-absorption effects [13], and the edge fluorescence spectrum: the spectrum of light incident on the solar cell. The re-absorption probability in thin film collectors for different concentrations of *R6G* is shown in Fig. 7; Fig. 8 shows the re-absorption probability for a liquid collector and different fluorophores.

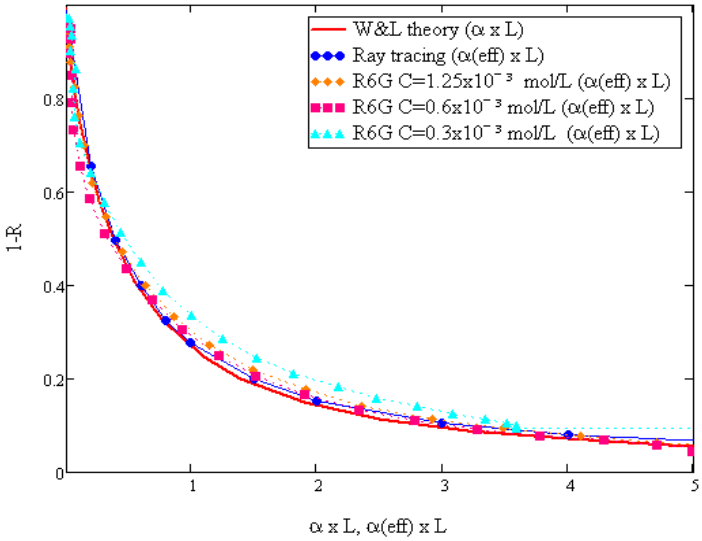

Fig. 7. (Colour online) Re-absorption probability for thin film collectors showing different concentrations of *R6G* in the film compared to the ray tracing simulations and the *W&L* model.

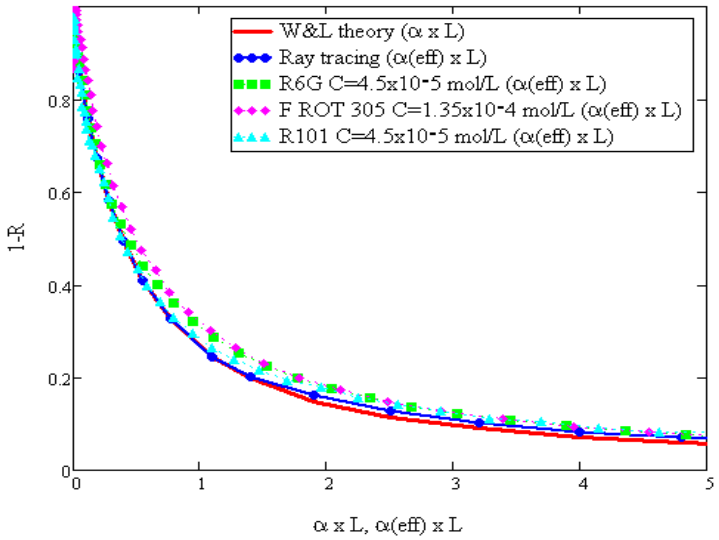

Fig. 8. (Colour online) Re-absorption probability obtained for liquid film collectors showing different dyes compared to the ray tracing simulations and *W&L* model.

Figs 7 and 8 clearly demonstrate the agreement between the simulations and the experiments. As predicted in the ray tracing simulations, the re-absorption probability is the same for both the thin film and liquid collectors. The results shown here are also independent of the type of fluorophore. Given the good fit between the theoretical and experimental results these results demonstrate that thin film collectors perform, for all purposes, identically to standard collectors when the refractive index of the substrate matches that of the active layer.

Several liquids and film with the same absorbance but different refractive index were prepared and characterised to assess the potential of the wave guiding properties of the thin film concept. All the experiments showed a drop in efficiency as soon as the refractive index of the fluorescent layer was different from the substrate, indicating a failure of the thin film "waveguide" concept. However, it is important to stress that changing the solvent to modify the refractive index of the fluorescent layer affects the surroundings of the fluorophore and hence the fluorescence properties of the dye (e.g. quantum yield). A direct comparison of the resulting efficiency using a range of different solvents is therefore not possible. This drop in efficiency was examined by ray-tracing simulations, as discussed in the following section.

6. THIN FILM COLLECTORS & THE "WAVEGUIDE" CONCEPT

To understand the drop in efficiency observed during the experiments, two variables, P and R were numerically determined using TracePro for different refractive indices of the film; in all cases the substrate is made of glass ($n=1.5$). As described in Table. 2, we modelled a thin film collector (*10mm x 10 mm*) with a film thickness of *200 μm* and a clear substrate of thickness *2 mm* with two possible configurations: (*i*) film on top of the substrate and (*ii*) substrate on top of the film. The materials composing the collector were perfectly clear, and the refractive index of the film varied from *1.1* to *2.7*.

The probability of emission outside the escape cone was given by studying the flux escaping from the edge of the collector (Fig. 9). The results were independent of the configuration of the collector studied, and were solely dependent on the refractive index of the fluorescent layer, as shown by the probability of emission outside the escape cone. Fig. 9 compares the analytical relation (3) (red thick line) and the modelling results (blue dots). For a refractive index of the fluorescent layer greater than *1.41* the ray tracing simulations shows a slightly better TIR trapping probability since they take into account reflection losses inside the escape cone.

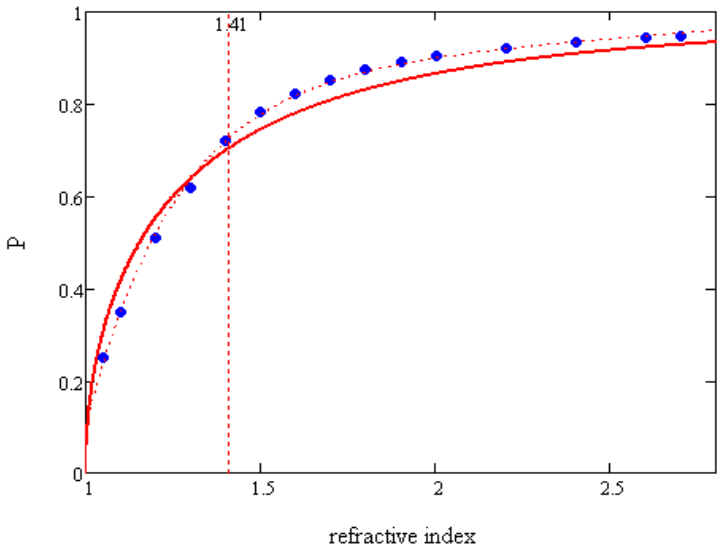

Fig. 9. Probability of emission outside the escape cone (*P*) given by relation (3) (red thick line) compared to ray tracing simulations (blue dots). The dotted red line correspond to a fit of the ray tracing simulations given by an exponential law *P(n)=A exp(B.n) + C exp(D.n)* where *A=0.81, B=0.06, C=-35.23* and *D=-3.836.*

It is interesting to note that the probability *P* decreases when the refractive index of the film is lower than *1.41*. This effect is due to the fact that for low refractive indices the aperture of the escape cone increases (*>45°*) and overlaps with the emission cone, decreasing the number of trapped photons. The results shown in Fig. 9 demonstrate that the light trapping probability is the same for thin film devices and standard collectors, as already discussed in Sec. 5.

A careful examination of light propagation in the device as function of different refractive indices of the film shows that light tends to propagate in the film if the refractive index of the film is different from that of the substrate. The inclusion of re-absorption in the simulations confirmed these results (Fig. 10), giving the lowest re-absorption profile for $n_a=n_s$. Any other refractive index combination leads to an increase of the re-absorption probability explaining the drop in efficiency observed during the experiments.

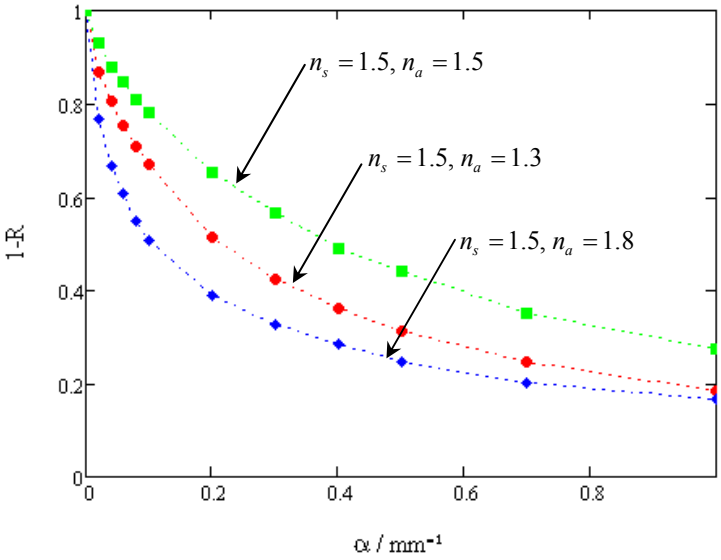

Fig. 10. Probability of reabsorption for different thin film refractive indices (n_a) coated on a glass substrate ($n_s=1.5$)

7. DISCUSSION AND CONCLUSION

Experiments and ray tracing simulations on liquid and thin film collectors demonstrated the validity and versatility of the Weber and Lambe model for re-absorption at high gain ratios. Triangular shaped collectors seem to be a promising shape for better photon collection. Despite the lower re-absorption probability shown by the triangular collector, high experimental efficiencies (in excess of *10%)*, are unlikely to be achieved with TIR based collectors because of the close link between Q_a and Q_c.

We have shown that thin film structures do not perform better than standard collectors. The optimum thin film configuration is reached when the refractive index of the film is the same as that of the substrate. In such configuration thin film devices can be treated as homogeneous devices with a resulting efficiency identical to plain collectors. High efficiency is then obtained for high refractive indices of the film and the substrate (15).

As already indicated in previous studies, our results highlight the fact that it is crucial to limit re-absorption (for example, by radiationless energy transfer) and to prevent the light escaping from the front of the collector (for example, using photonic band stop filters). With a good photon management the theoretical efficiency of a collector can approach *90%* for appreciable gain factors, compared to *58%* for TIR based collectors [2-3, 16].

It is my pleasure to acknowledge many stimulating discussions with my colleagues and friends F. Pace and L. Danos. I would also like to thank the individuals from the industry cooperating with us, especially, B. Calt (TracePro) for a free license, P. Bailey (Hellma) for the help with the collector design, L. Lyons (Bentham) for his help with the system calibration and D. Turner (BASF) for kindly donating the lumogen dyes, A. Moshar (Asylum Research UK) for the help with AFM roughness measurement and A. Kuhle (SPIP) for the roughness analysis. Not to forget to forget P. Kittidachachan for the help with the fluorescence measurements reported in Fig. 7 of this publication.

REFERENCES

[1] Weber, W.H., Lambe, J., "Luminescent greenhouse collector for solar radiation," App. Opt. 15(10), 2299-2300 (1976).
[2] Kittidachachan, P., Danos, L., Meyer, T.J.J., Alderman, N., Markvart, T., "Photon collection efficiency of fluorescent solar collectors," Chimia 61(12), 1-7 (2007).
[3] Markvart, T., "Detailed balance method for ideal single-stage fluorescent collectors," J. App. Phys 99, 026101 (2006).
[4] Kennard, E.H., "On the interaction of radiation with matter and on fluorescent exciting power," Phys review 28, 673-683 (1926).
[5] Batchelder, J. S., Zewail, A.H., Cole, T., "Luminescent Solar Concentrators (LSC)," 24th Proc SPIE 248, 105-108 (1980).
[6] Batchelder, J. S., Zewail, A.H., Cole, T., "Luminescent Solar Concentrators (LSC) I: Theory of Operation," App. Opt.18, 3090-3109 (1979).
[7] Batchelder, J. S., Zewail, A.H., Cole, T., "Luminescent Solar Concentrators (LSC) II: Experimental and theoretical analysis of their possible efficiencies," App. Opt. 20(21), 3733-3754 (1981).
[8] Stover, J.C., [Optical scattering: measurements and analysis], SPIE The international society for optical engineering, Washington, (1995).
[9] Harvey, J.E., [Light-scattering properties of optical surfaces], Ph.D. dissertation, U. Arizona, (1976).
[10] Deutsches Institut Fur Normung E.V. (German National Standard). DIN 58170-54, 2 (1980).
[11] Goetzberger, A., Greubel, W., "Solar energy conversion with fluorescent collectors," J. of App. Phys 14, 123-139 (1977).
[12] Rapp, C.F., Boling, N.L., "Luminescent solar concentrators," 13th Proc IEEE, pp. 690-693 (1978).
[13] Lakowicz, J.R., [Principle of fluorescent spectroscopy], Springer Science, Baltimore, (2006).
[14] Meyer, T.J.J., Markvart, T., "The chemical potential of fluorescent light," 23st Proc EU PVSEC, 399-403 (2008).
[15] Currie, M.J., Mapel, J.K., Heidel, T.D., Goffri, S., Baldot, M.A., "High-efficiency organic solar concentrators for photovoltaics," Science 321(226), 226-228 (2008).
[16] Rau, U., Einsele, F., Glaeser, G.C., "Efficiency limits of photovoltaic fluorescent collectors," App. Phys. Lett. 87 (17), 171101 (2005).